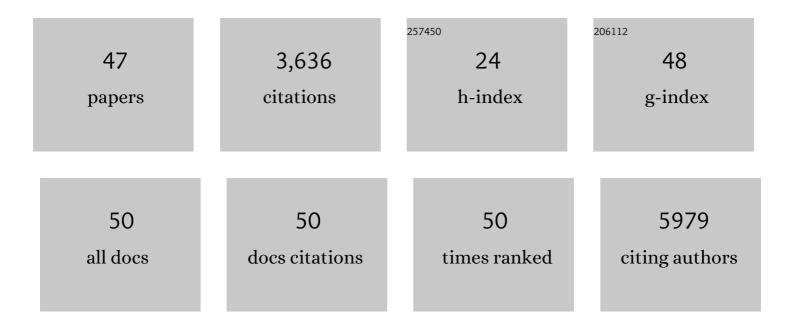
Yi-Sheng Liu

List of Publications by Year in descending order

Source: https://exaly.com/author-pdf/2914727/publications.pdf Version: 2024-02-01



VI-SHENC LIU

#	Article	IF	CITATIONS
1	Charge-compensation in 3d-transition-metal-oxide intercalation cathodes through the generation of localized electron holes on oxygen. Nature Chemistry, 2016, 8, 684-691.	13.6	898
2	Probing the Optical Property and Electronic Structure of TiO ₂ Nanomaterials for Renewable Energy Applications. Chemical Reviews, 2014, 114, 9662-9707.	47.7	422
3	Efficient electrically powered CO2-to-ethanol via suppression of deoxygenation. Nature Energy, 2020, 5, 478-486.	39.5	363
4	Anion Redox Chemistry in the Cobalt Free 3d Transition Metal Oxide Intercalation Electrode Li[Li _{0.2} Ni _{0.2} Mn _{0.6}]O ₂ . Journal of the American Chemical Society, 2016, 138, 11211-11218.	13.7	271
5	Oxygen evolution reaction over catalytic single-site Co in a well-defined brookite TiO2 nanorod surface. Nature Catalysis, 2021, 4, 36-45.	34.4	189
6	Graphene oxide/metal nanocrystal multilaminates as the atomic limit for safe and selective hydrogen storage. Nature Communications, 2016, 7, 10804.	12.8	178
7	Carbon doping switching on the hydrogen adsorption activity of NiO for hydrogen evolution reaction. Nature Communications, 2020, 11, 590.	12.8	170
8	Copper adparticle enabled selective electrosynthesis of n-propanol. Nature Communications, 2018, 9, 4614.	12.8	153
9	Efficient Hydrogen Production from Methanol Using a Single-Site Pt ₁ /CeO ₂ Catalyst. Journal of the American Chemical Society, 2019, 141, 17995-17999.	13.7	114
10	A nature-inspired hydrogen-bonded supramolecular complex for selective copper ion removal from water. Nature Communications, 2020, 11, 3947.	12.8	86
11	Electronic Structure, Optoelectronic Properties, and Photoelectrochemical Characteristics of γ-Cu ₃ V ₂ O ₈ Thin Films. Chemistry of Materials, 2017, 29, 3334-3345.	6.7	60
12	CuBi ₂ O ₄ : Electronic Structure, Optical Properties, and Photoelectrochemical Performance Limitations of the Photocathode. Chemistry of Materials, 2021, 33, 934-945.	6.7	45
13	Reversible Electrochemical Interface of Mg Metal and Conventional Electrolyte Enabled by Intermediate Adsorption. ACS Energy Letters, 2020, 5, 200-206.	17.4	44
14	An ultra-high vacuum electrochemical flow cell for in situ/operando soft X-ray spectroscopy study. Review of Scientific Instruments, 2014, 85, 043106.	1.3	43
15	Electronic Structure and Performance Bottlenecks of CuFeO ₂ Photocathodes. Chemistry of Materials, 2019, 31, 2524-2534.	6.7	43
16	Correlation-driven eightfold magnetic anisotropy in a two-dimensional oxide monolayer. Science Advances, 2020, 6, eaay0114.	10.3	43
17	Reversible dehydrogenation and rehydrogenation of cyclohexane and methylcyclohexane by single-site platinum catalyst. Nature Communications, 2022, 13, 1092.	12.8	41
18	Nanoconfinement of Molecular Magnesium Borohydride Captured in a Bipyridine-Functionalized Metal–Organic Framework. ACS Nano, 2020, 14, 10294-10304.	14.6	40

YI-SHENG LIU

#	Article	IF	CITATIONS
19	Atomically Thin Interfacial Suboxide Key to Hydrogen Storage Performance Enhancements of Magnesium Nanoparticles Encapsulated in Reduced Graphene Oxide. Nano Letters, 2017, 17, 5540-5545.	9.1	37
20	Enhanced and stabilized hydrogen production from methanol by ultrasmall Ni nanoclusters immobilized on defect-rich h-BN nanosheets. Proceedings of the National Academy of Sciences of the United States of America, 2020, 117, 29442-29452.	7.1	34
21	Full Energy Range Resonant Inelastic X-ray Scattering of O ₂ and CO ₂ : Direct Comparison with Oxygen Redox State in Batteries. Journal of Physical Chemistry Letters, 2020, 11, 2618-2623.	4.6	30
22	A Mechanistic Analysis of Phase Evolution and Hydrogen Storage Behavior in Nanocrystalline Mg(BH ₄) ₂ within Reduced Graphene Oxide. ACS Nano, 2020, 14, 1745-1756.	14.6	29
23	A lithium-sulfur battery with a solution-mediated pathway operating under lean electrolyte conditions. Nano Energy, 2020, 76, 105041.	16.0	25
24	Multimodal characterization of solution-processed Cu ₃ SbS ₄ absorbers for thin film solar cells. Journal of Materials Chemistry A, 2018, 6, 8682-8692.	10.3	24
25	Elucidating the mechanism of MgB ₂ initial hydrogenation via a combined experimental–theoretical study. Physical Chemistry Chemical Physics, 2017, 19, 22646-22658.	2.8	23
26	X-ray spectroscopies studies of the 3d transition metal oxides and applications of photocatalysis. MRS Communications, 2017, 7, 53-66.	1.8	22
27	Excess Lithium in Transition Metal Layers of Epitaxially Grown Thin Film Cathodes of Li ₂ MnO ₃ Leads to Rapid Loss of Covalency during First Battery Cycle. Journal of Physical Chemistry C, 2019, 123, 28519-28526.	3.1	19
28	In-situ/operando X-ray absorption spectroscopic investigation of the electrode/electrolyte interface on the molecular scale. Surface Science, 2020, 702, 121720.	1.9	19
29	Strong O 2p–Fe 3d Hybridization Observed in Solution-Grown Hematite Films by Soft X-ray Spectroscopies. Journal of Physical Chemistry B, 2018, 122, 927-932.	2.6	18
30	Nanoscale Mg–B <i>via</i> Surfactant Ball Milling of MgB ₂ : Morphology, Composition, and Improved Hydrogen Storage Properties. Journal of Physical Chemistry C, 2020, 124, 21761-21771.	3.1	17
31	Spontaneous dynamical disordering of borophenes in MgB2 and related metal borides. Nature Communications, 2021, 12, 6268.	12.8	14
32	Inâ€Situ/Operando Xâ€ray Characterization of Metal Hydrides. ChemPhysChem, 2019, 20, 1261-1271.	2.1	12
33	Probing calcium solvation by XAS, MD and DFT calculations. RSC Advances, 2020, 10, 27315-27321.	3.6	12
34	Runaway Carbon Dioxide Conversion Leads to Enhanced Uptake in a Nanohybrid Form of Porous Magnesium Borohydride. Advanced Materials, 2019, 31, e1904252.	21.0	10
35	Investigating possible kinetic limitations to MgB2 hydrogenation. International Journal of Hydrogen Energy, 2019, 44, 31239-31256.	7.1	10
36	Soft x-ray spectroscopy of high pressure liquid. Review of Scientific Instruments, 2018, 89, 013114.	1.3	9

YI-SHENG LIU

#	Article	IF	CITATIONS
37	Sugar-alcohol@ZIF nanocomposites display suppressed phase-change temperatures. Journal of Materials Chemistry A, 2020, 8, 23795-23802.	10.3	9
38	Deciphering the Solvent Effect for the Solvation Structure of Ca ²⁺ in Polar Molecular Liquids. Journal of Physical Chemistry B, 2020, 124, 3408-3417.	2.6	8
39	The influence of LiH and TiH2 on hydrogen storage in MgB2 II. XPS study of surface and near-surface phenomena. International Journal of Hydrogen Energy, 2022, 47, 403-419.	7.1	8
40	Phonon Dispersion Relation of Bulk Boron-Doped Graphitic Carbon. Journal of Physical Chemistry C, 2020, 124, 23027-23037.	3.1	7
41	Disparate Exciton-Phonon Couplings for Zone-Center and Boundary Phonons in Solid-State Graphite. Physical Review Letters, 2020, 125, 116401.	7.8	7
42	Factors Defining the Intercalation Electrochemistry of CaFe ₂ O ₄ -Type Manganese Oxides. Chemistry of Materials, 2020, 32, 8203-8215.	6.7	6
43	Additive Destabilization of Porous Magnesium Borohydride Framework with Coreâ€6hell Structure. Small, 2021, 17, e2101989.	10.0	6
44	The influence of LiH and TiH2 on hydrogen storage in MgB2 I: Promotion of bulk hydrogenation at reduced temperature. International Journal of Hydrogen Energy, 2022, 47, 387-402.	7.1	6
45	A facile route for the synthesis of heterogeneous crystal structures in hierarchical architectures with vacancy-driven defects <i>via</i> the oriented attachment growth mechanism. Journal of Materials Chemistry A, 2018, 6, 10663-10673.	10.3	4
46	Intercalation of Mg into a Few-Layer Phyllomanganate in Nonaqueous Electrolytes at Room Temperature. Chemistry of Materials, 2020, 32, 6014-6025.	6.7	3
47	In situ/operando soft x-ray spectroscopy of chemical interfaces in gas and liquid environments. MRS Bulletin, 2021, 46, 747-754.	3.5	2